Journal of Coastal Research	14	3	917–932	Royal Palm Beach, Florida	Summer 1998

On Modelling Wind-Waves in Shallow and Fetch Limited Areas Using the Method of Holthuijsen, Booij and Herbers

H.K. Johnson

Danish Hydraulic Institute
Agern Allé 5
DK-2970 Hørsholm, Denmark

ABSTRACT

JOHNSON, H.K., 1998. On modelling wind-waves in shallow and fetch limited areas using the method of Holthuijsen, Booij and Herbers. *Journal of Coastal Research,* 14(3), 917–932 . Royal Palm Beach (Florida), ISSN 0749-0208.

A parametric discrete spectral model, MIKE 21 NSW, based on the equations presented by HOLTHUIJSEN, BOOIJ and HERBERS, 1989 (HBH) is used to compute the growth of wind-waves in the shallow and fetch limited waters off the coast of Lolland, Denmark. A simple procedure is used to obtain the HBH wind-wave growth coefficients from empirical deep water wave growth formula without the need of tuning. Simulations are carried out to assess the influence of wind-wave growth source functions, bottom friction, wave breaking and assumed spectral shape. Results indicate that for this limited fetch (about 20 km) in relatively shallow water (depths about 3–4m near measurement locations), the locally generated significant wave heights are not sensitive to bottom friction and depth induced wave breaking. Of the 5 wave growth formulas investigated, the best results were obtained using HBH coefficients corresponding to the SPM(1984) or the KAHMA & CALKOEN(1994) formulas. The results show that the method performs much better for calculating waves in shallow and fetch limited situations than a direct calculation with the SPM (1984) shallow water formula.

ADDITIONAL INDEX WORDS: *Locally generated waves, parametric spectral model, fetch limited waves.*

INTRODUCTION

In many practical situations, it is necessary to predict the locally generated wind-waves in shallow and fetch limited waters. This is the case in closed or semi-enclosed waters such as lagoons, lakes *etc.* At the present stage, the knowledge of this phenomenon is limited. For many years, the tool has been the *Shore Protection Manual* shallow water wave prediction equations (SPM 1973, 1984, hereafter referred to as SPM73 and SPM84 respectively) or other wave prediction equations empirically derived from field data. Within the last 5–10 years, numerical models including wind-wave generation and shallow water processes are gradually being used. For example, the model HISWA presented by Holthuijsen, Booij and Herbers (hereafter referred to as HBH) and MIKE 21[1] Nearshore Spectral Wind-wave model (NSW) which is based on the same equations as HISWA. However, the applicability of this model for wind-wave generation in shallow waters has not been widely documented against measured data. This paper is of significant interest to coastal researchers because it validates an important tool for wave hindcasting.

In the equations presented by HBH, which is implemented in NSW, the input source function is formulated using empirical deep water wave prediction equations with the same dimensionless form as in SPM84. It is noted that this method of formulating source functions using empirical deep water wave prediction formulas is not a theoretically rigorous method of describing wind-wave generation because of the parameterizations inherent in this approach. One of the simplifications in this approach is the assumption of a single-peaked spectrum. The implication of this is that mixed sea (locally generated waves and swell (longer period waves generated far from the location)) conditions can-not be simulated with the method. This requires the use of more advanced models, such as the third generation wave model, WAM, (KOMEN *et al.*, 1994) which describes the physics of wind-wave generation and transformation of the wave spectra using a more fundamental approach. However, using the WAM model is prohibitively expensive in coastal situations where the need to resolve important bathymetric details usually lead to small grid spacings in many cases and thus relatively large models (in terms of number of grid points). At the level of detail in the WAM model, there are still several unsolved problems associated with modelling waves in shallow water. Thus, a parameterized spectral approach such as used by HBH is a compromise between using a fully spectral description and simple empirical wave prediction equations that are unable to incorporate the influence of refraction, shoaling, wave breaking etc. Hence, this method should be thought of as a pragmatic approach, which is however not valid in mixed sea/swell conditions.

96106 received 20 September 1996; accepted in Revision 24 February 1997.

[1] *MIKE 21 is a 2D modelling software developed at the Danish Hydraulic Institute.*

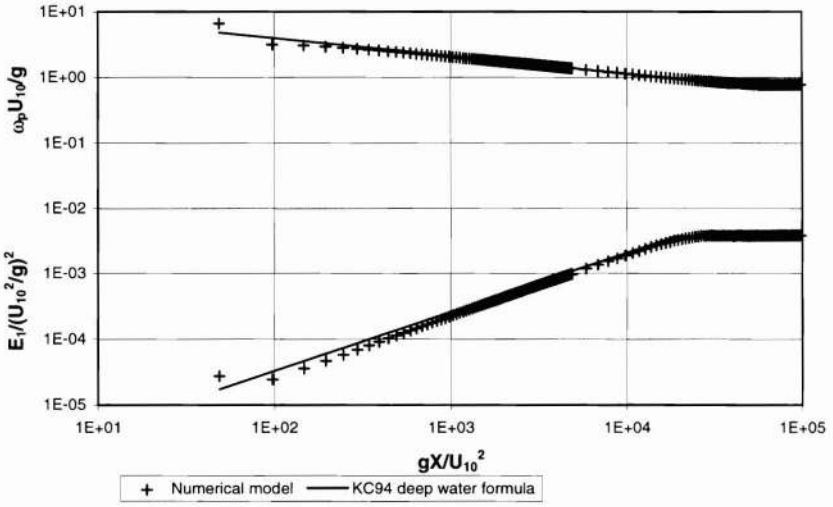

Figure 1. Deep water wind wave growth curves according to KAHMA and CALKOEN (1994) (full lines), Numerical model computations (crosses).

This paper describes the application of MIKE 21 NSW model to compute the growth of wind-waves in the shallow and fetch limited waters off the coast of Lolland, Denmark. Since the waves in this application are locally generated, this makes it possible to focus on the mechanisms affecting local wind-wave generation in the model. In this respect, the influence of wind-wave growth source function, bed friction, wave breaking and assumed JONSWAP spectral shape are examined. The outline of this paper is as follows: In section 2, the governing equations are presented, the measured data is presented in section 3, followed by the analysis with the model in section 4 and finally a summary of the work done and conclusions are presented in section 5.

GOVERNING EQUATIONS

MIKE 21 NSW is a stationary, parameterized spectral wind-wave model which describes the propagation, growth and decay of short-period and short-crested waves in nearshore areas. The model takes into account the effects of refraction and shoaling due to varying depth, local wind generation, energy dissipation due to bottom friction and wave breaking, and the effect of wave-current interaction.

The theoretical formulation for the model was given by Holthuijsen, Booij and Herbers (HBH). The governing equations solved are:

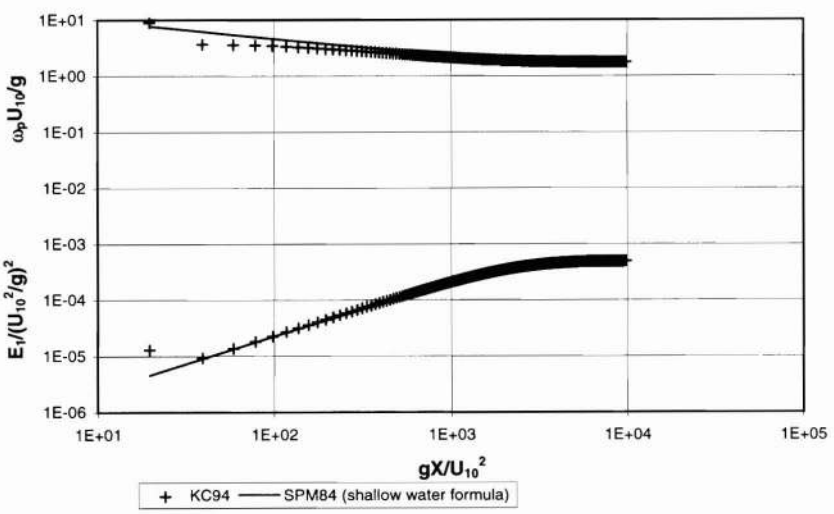

Figure 2. Shallow water wind wave growth curves according to Shore Protection Manual (1984) (full lines), Numerical model computations (crosses). The shallow water computations is carried out for a water depth of 5 m, and wind speed U_{10} = 10 m/s corresponding to U_a = 12 m/s used in the SPM84 equations.

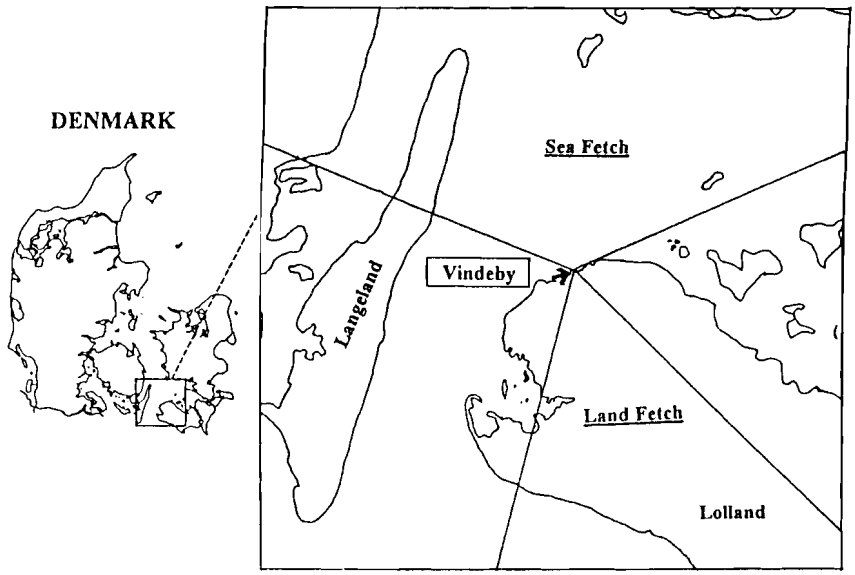

Figure 3. Location of Vindeby, Denmark (from BARTHELMIE *et al.*, 1994).

$$\frac{\partial(c_{gx}m_0)}{\partial x} + \frac{\partial(c_{gy}m_0)}{\partial y} + \frac{\partial(c_\theta m_0)}{\partial \theta} = T_0 \quad (1)$$

$$\frac{\partial(c_{gx}m_1)}{\partial x} + \frac{\partial(c_{gy}m_1)}{\partial y} + \frac{\partial(c_\theta m_1)}{\partial \theta} = T_1 \quad (2)$$

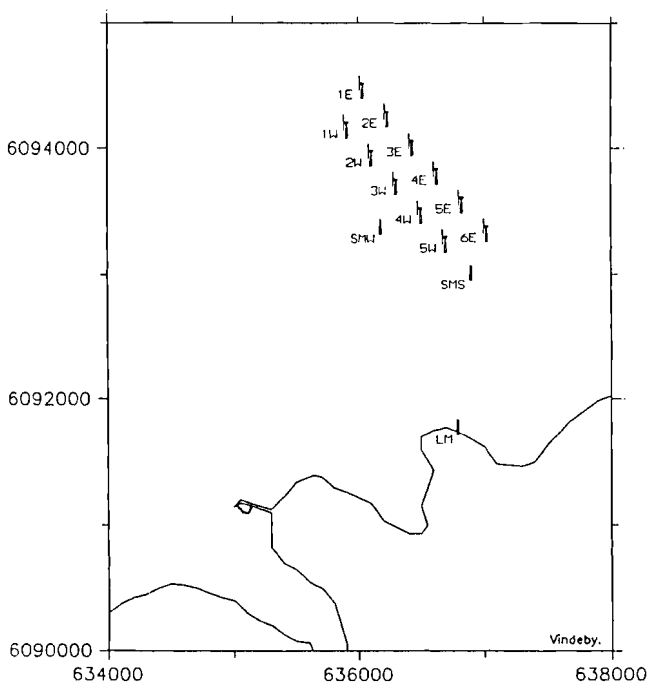

Figure 4. The configuration of the wind farm and positions of the masts at Vindeby (from BARTHELMIE *et al.*, 1994). Distances in meters.

where $m_0(x,y,\theta)$ and $m_1(x,y,\theta)$ are respectively the zeroth and first moment of the action spectrum, c_{gx} and c_{gy} are the x- and y-components of the group velocity, c_θ is the propagation speed representing change of wave action in θ-direction, x and y are Cartesian coordinates, θ is the direction of wave propagation and $T_0(x, y, \theta)$ and $T_1(x, y, \theta)$ are source terms based on the action spectrum. The propagation speeds c_{gx}, c_{gy} and c_θ are obtained using linear wave theory.

The moments $m_n(\theta)$ are defined as:

$$m_n(\theta) = \int_0^\infty \omega^n A(\omega, \theta)\, d\omega \quad (3)$$

where ω is the absolute frequency and A is the spectral wave action density.

The left hand side of Eqs. 1 and 2 take into account the effect of refraction and shoaling. The source terms T_0 and T_1 take into account the effect of local wind generation and energy dissipation due to bottom friction and wave breaking.

HBH showed that the source terms T_0 and T_1, can be conveniently expressed in terms of the source functions for the wave energy, $S_E(x, y, \theta)$ and the mean frequency of the action spectrum, $S_\omega(x, y, \theta)$. They obtained:

$$T_1(\theta) = \frac{\omega_0}{\sigma_0} S_E(\theta); \qquad S_E(\theta) = \frac{dE_0}{dt} \quad (4)$$

$$T_0(\theta) = \frac{1}{\sigma_0}\left\{S_E(\theta) - \frac{E_0(\theta)}{\omega_0} S_\omega(\theta)\right\}; \qquad S_\omega(\theta) = \frac{d\omega_0}{dt} \quad (5)$$

where ω_0 is the absolute action averaged mean frequency, σ_0 is the intrinsic action averaged mean frequency ($\omega_0 = \sigma_0 + \mathbf{k}.\mathbf{U}$, where k is the wave number vector and U is the current vector), $E_0(\theta)$ is the wave energy defined as $\int E(\omega, \theta)\, d\omega$. S_ω is obtained from the source function for the energy averaged mean frequency using $S_\omega = \omega_0/\Omega_0\, S_\Omega$, where Ω_0 is the energy

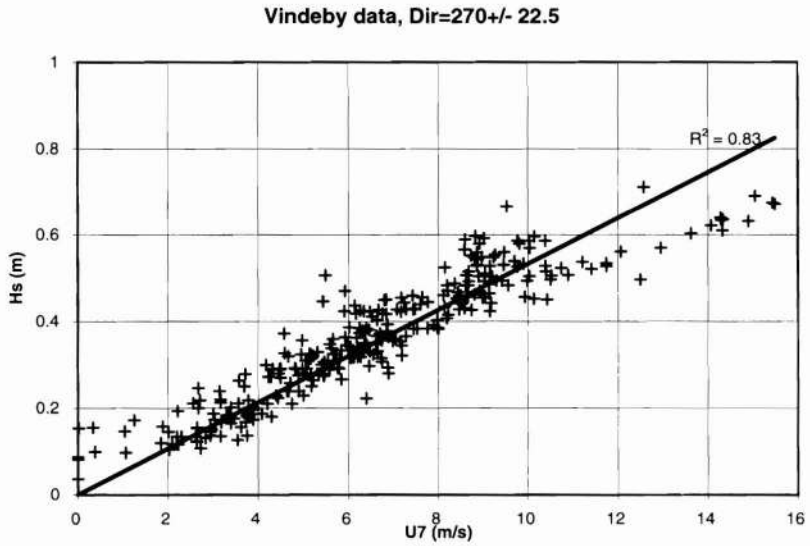

Figure 5. Vindeby data: Correlation between wave height and wind speed.

averaged mean frequency. In their model, HBH used the ratio $\omega_0/\Omega_0 = 0.92$, which corresponds to the mean JONSWAP spectrum (HASSELMANN *et al.*, 1973). This is also used in this study.

The source terms due to bottom friction dissipation in HBH is based on the quadratic friction law to represent bottom shear stress and assumes a Rayleigh distribution of wave heights in the random wave train. The starting point for the derivation of the source terms for bottom friction is DINGEMANS (1983) expression for dissipation in unidirectional random waves with Rayleigh distributed wave heights with one frequency, ω.

$$\left(\frac{dE}{dt}\right)_{bottom} = -\frac{1}{8\pi^{1/2}}\frac{C_{fw}}{g}\frac{\omega^3}{\sinh^3(kd)}H_{rms}^3 \qquad (6)$$

where C_{fw} is a friction coefficient, which can be obtained from the geometrical bed roughness k_N, using the expression by JONSSON (1966) for wave friction factors. HBH derived the bottom friction source terms $S_E(x, y, \theta)$ and $S_\omega(x, y, \theta)$ for the more general condition of directional random waves in the presence of currents.

The source term due to wave breaking is based on the theory of BATTJES and JANSSEN (1979). In this theory, the distribution of wave heights is assumed to follow a truncated Rayleigh distribution (truncated at the maximum wave height, H_m with waves exceeding H_m assumed to be breaking waves) while the rate of dissipation is modelled using an analogy with dissipation in a bore. The value of H_m is obtained using a MICHE (1944) type breaking criterion:

$$H_m = \gamma_1/k \tanh(\gamma_2 k d/\gamma_1) \qquad (7)$$

where k is the wave number based on the energy averaged mean frequency, Ω_o, d is water depth, γ_1 and γ_2 are free parameters. γ_1 controls the maximum wave steepness in deep water (and thus controls steepness related wave breaking) while γ_2 controls the maximum wave height in shallow water (and thus controls depth-induced wave breaking). Thus, this wave breaking dissipation model includes both deep-water breaking (steepness related) and shallow water breaking (depth-induced). Where we have investigated only shallow water wave breaking, the maximum wave height is simply taken as: $H_m = \gamma_2 d$.

The source terms for local wind generation are obtained from empirical deep water wave growth equations. The total wave energy, E_1 (defined as $H_{m0}^2/16$, where H_{m0} is significant wave height) and the energy averaged mean frequency, Ω_1, are formulated in terms of duration using dimensionless quantities (the duration t, is defined as the equivalent duration required to generate such a wave, for a stationary wind blowing along the fetch from t = 0). These equations can be written as:

$$\bar{E}_1 = a\bar{t}^b \quad \text{for } \bar{t} < \bar{t}_{mE} \qquad (8a)$$

$$\bar{E}_1 = a\bar{t}_{mE}^b \quad \text{for } \bar{t} \geq \bar{t}_{mE} \qquad (8b)$$

$$\bar{\Omega} = c\bar{t}^d \quad \text{for } \bar{t} < \bar{t}_{m\Omega} \qquad (9a)$$

$$\bar{\Omega} = c\bar{t}_{m\Omega}^d \quad \text{for } \bar{t} \geq \bar{t}_{m\Omega} \qquad (9b)$$

where t_m is the equivalent duration at full development and $\bar{E}_1$, $\bar{\Omega}_1$ and $\bar{t}$ are dimensionless forms of E_1, Ω_1 and t using wind speed, U and acceleration due to gravity, g. The coefficients, a, b, c, d, t_{mE} and $t_{m\Omega}$ are fitted to selected empirical deep water, fetch limited wave growth formulas.

The source terms are evaluated separately for each direction, using the concept of "equivalent" total energy and mean frequency along each discrete direction, $E^*(\theta)$, $\Omega^*(\theta)$. $E^*(\theta)$ is calculated as $E^*(\theta) = E_o(\theta)/D_{wind}(\theta)$, where $D_{wind}(\theta)$ is a $\cos^2(\theta - \theta_{wind})$ directional spreading function and $E_o(\theta)$ is the energy along the discrete direction considered, while $\Omega^*(\theta) = \Omega_o(\theta)$. The equivalent durations are found from Eqs. 8–9 using $E^*(\theta)$

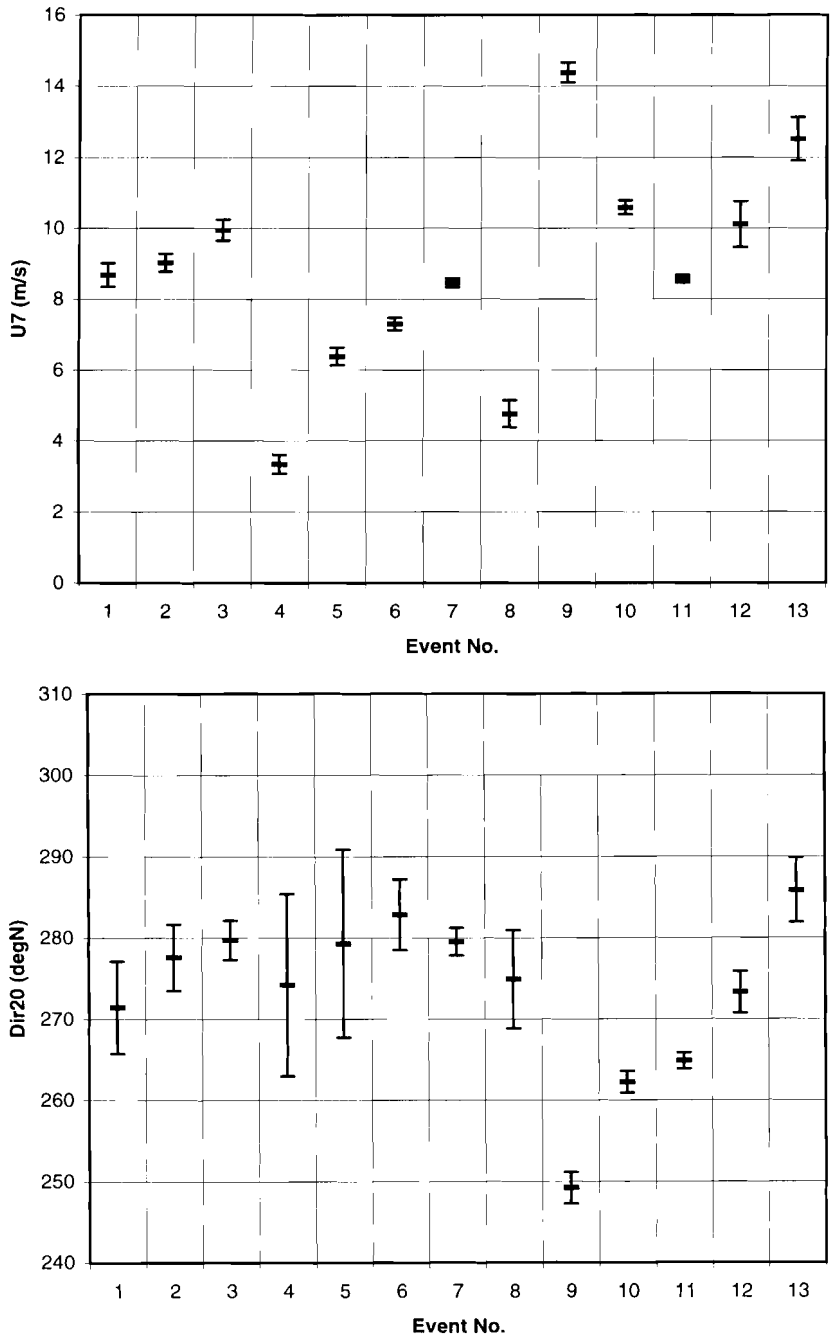

Figure 6. Illustration of measured wind data for the thirteen events. (a) wind speed, (b) wind direction.

and $\Omega^*(\theta)$, from which $S_{E'}(\theta)$ and $S_{\Omega'}(\theta)$ are determined. Thereafter, the source functions $S_E(\theta)$ is found as: $S_E(\theta)=S_{E'}(\theta)*D_{wind}(\theta)$, while $S_{\Omega'}(\theta)$ is assumed to be independent of θ. Thus $S_\Omega(\theta) = S_{\Omega'}(\theta)$. Finally, a relaxation factor is applied to $S_\Omega(\theta)$ which forces the value of $\Omega_o(\theta)$ towards the directional equivalent of the universal relationship: $\bar{\Omega}_1 = e\,\bar{E}_1'$. Additional details about the description of the source terms can be found in HBH.

There are basically 2 ways of obtaining the coefficients in Eqs. 8 and 9. One way is to tune the coefficients until it reproduces the fetch limited wave growth for the specified empirical wave growth prediction equation under ideal conditions. It appears that this is what was done in HBH, and they obtained the following coefficients for the SPM73 deep water wave growth equation: a = 1.44×10^{-8}; b = 1.12; c = 43.59; d = −1/3 and $t_{mE} = t_{m\Omega} = 6.6\times10^4$. In obtaining the above

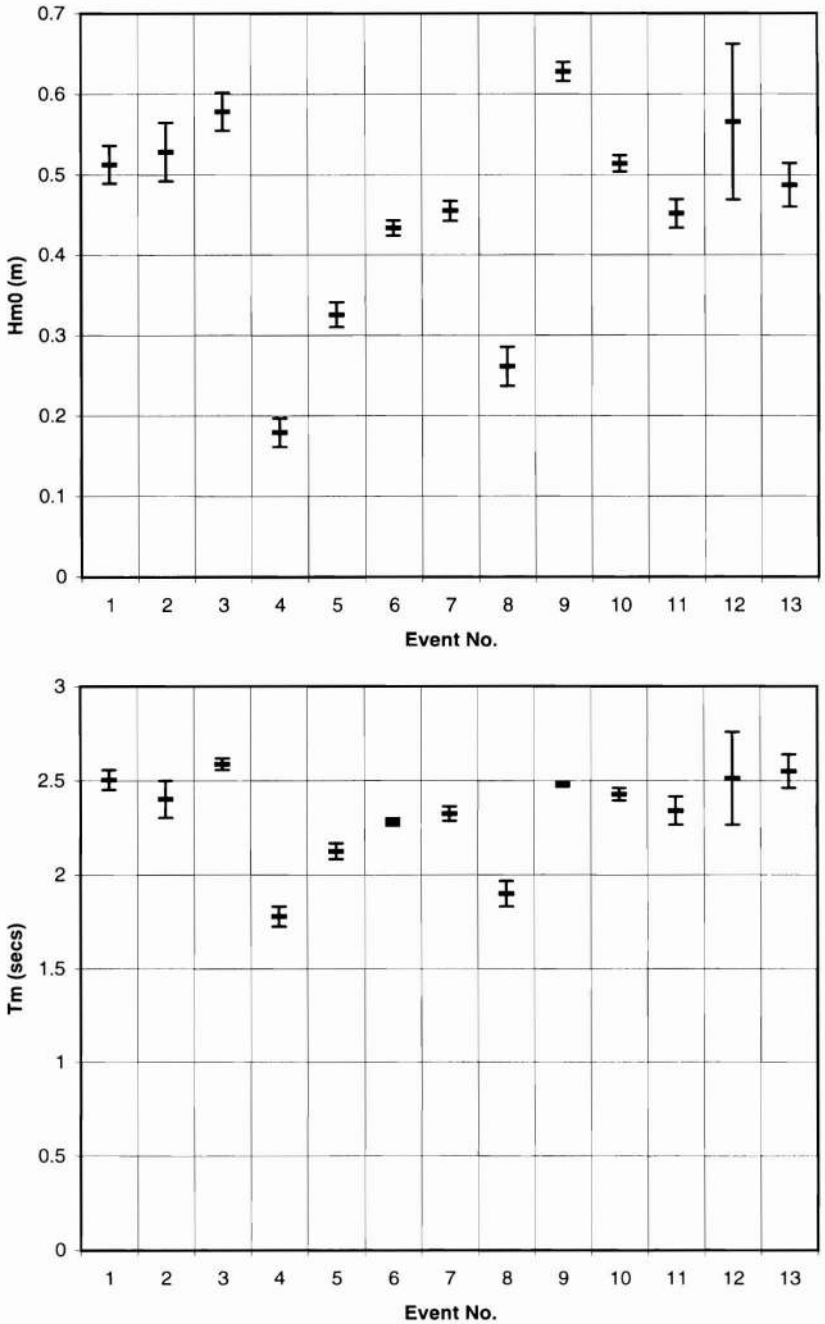

Figure 7. Illustration of measured wave data for the thirteen events. (a) Significant wave height, H_{mo}, (b) Mean wave period, T_m.

coefficients, they assumed that the significant wave period, T_s is related to the energy averaged mean period, T_m using $T_s = 1.2\ T_m$.

An alternative way to obtain the above coefficients without the need for additional tuning is to extract the coefficients directly from the information on deep water fetch limited wave growth available from the literature. This is usually written as:

$$\tilde{E} = a_1 \tilde{x}^{b_1} \tag{10}$$

$$\tilde{\omega}_p = c_1 \tilde{x}^{d_1} \tag{11}$$

where $\tilde{x}$ is dimensionless fetch. The equivalent duration, t, for waves to be limited by a given fetch, x is given by:

$$t = \int_0^x \frac{dx}{c_g} \tag{12}$$

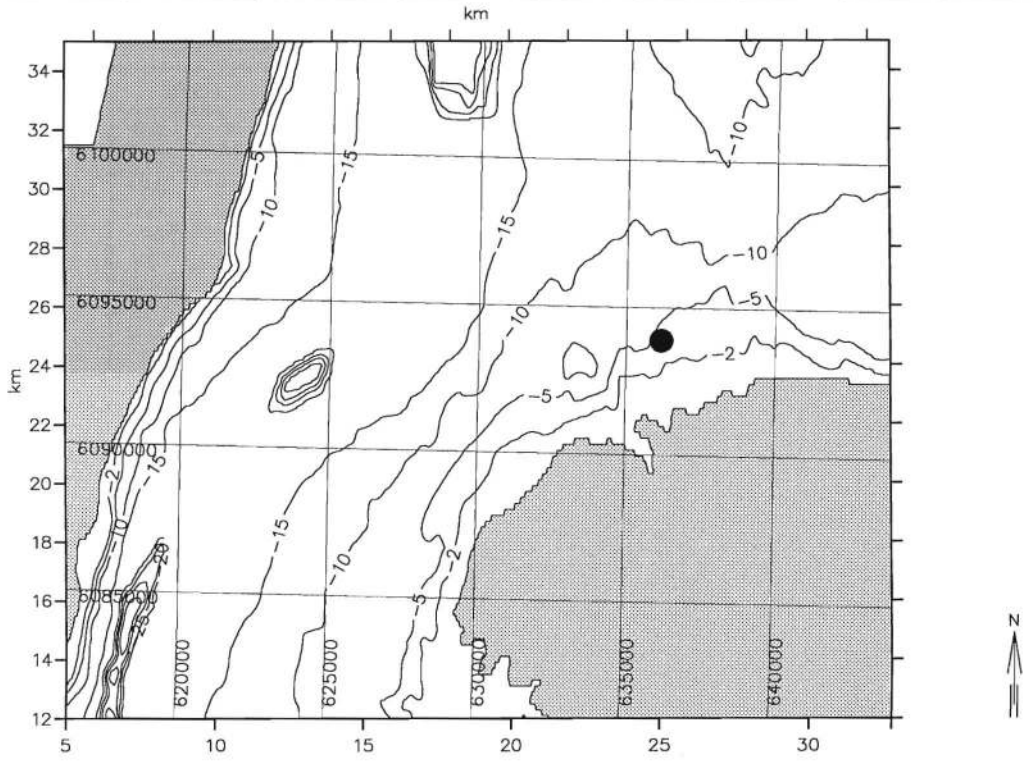

Figure 8. Digitized bathymetry used in MIKE 21 NSW model simulations. The superimposed net is annotated with the same coordinate system as in Figure 4. Heavy black dot indicates wave measurement location.

Now, assuming the random waves travel with a deep water group velocity corresponding to the energy averaged frequency, $\Omega = \beta\,\omega_p$ (where β is a constant depending on the assumed shape of the spectrum, β=1.2 for mean JONSWAP), the dimensionless equivalent duration can be written as:

$$\bar{t} = \frac{2\beta c_1}{1 + d_1}\bar{x}^{(1+d_1)} \tag{13}$$

Using Eq. 13, the fetch relations of Eqs. 10 and 11 can be rewritten as:

Table 1. *Coefficients used in the source functions for wind growth. For the SPM73 equations, the following power functions are fitted:* $\bar{E}_1 = 8.961 .10^{-7}\,\bar{x}^{0.803}$, $\bar{\omega}_p = 9.508\,\bar{x}^{0.2245}$ *with correlation coefficient of approximately 1. The wind speed used is the wind speed at 10 m elevation,* U_{10} *except in the case of SPM84 where the wind stress factor* $U_a = 0.71\,U_{10}^{1.23}$ *is used.*

	SPM73	SPM84	Kahma & Calkoen (1994)
a	2.70×10^{-8}	2.27×10^{-10}	4.75×10^{-9}
b	1.036	1.500	1.233
c	30.37	234.80	67.26
d	−0.2895	−0.50	−0.37
t_{mE}	9.09×10^4	6.79×10^4	6.00×10^4
$t_{m\Omega}$	17.15×10^4	6.42×10^4	10.69×10^4

$$\bar{E} = a_1\left(\frac{1 + d_1}{2\beta c_1}\right)^{b_1/1+d_1}\bar{t}^{b_1/1+d_1} \tag{14}$$

$$\bar{\omega}_p = c_1\left(\frac{1 + d_1}{2\beta c_1}\right)^{d_1/1+d_1}\bar{t}^{d_1/1+d_1} \tag{15}$$

Now, using the relationship between the energy averaged frequency Ω and the peak frequency ω_p, ie. $\Omega = \beta\,\omega_p$, Eq. 15 can be rewritten as:

$$\bar{\Omega} = \beta c_1\left(\frac{1 + d_1}{2\beta c_1}\right)^{d_1/1+d_1}\bar{t}^{d_1/1+d_1} \tag{16}$$

Comparing Eqs. 14 and 16 with Eqs. 8a and 9a respectively, the coefficients a, b, c, and d can be written as follows:

$$a = a_1\left(\frac{1 + d_1}{2\beta c_1}\right)^{b_1/1+d_1} \tag{17a}$$

$$b = \frac{b_1}{1 + d_1} \tag{17b}$$

$$c = \beta c_1\left(\frac{1 + d_1}{2\beta c_1}\right)^{d_1/1+d_1} \tag{17c}$$

$$d = \frac{d_1}{1 + d_1} \tag{17d}$$

The equivalent maximum duration at full development (t_{mE}, $t_{m\Omega}$)

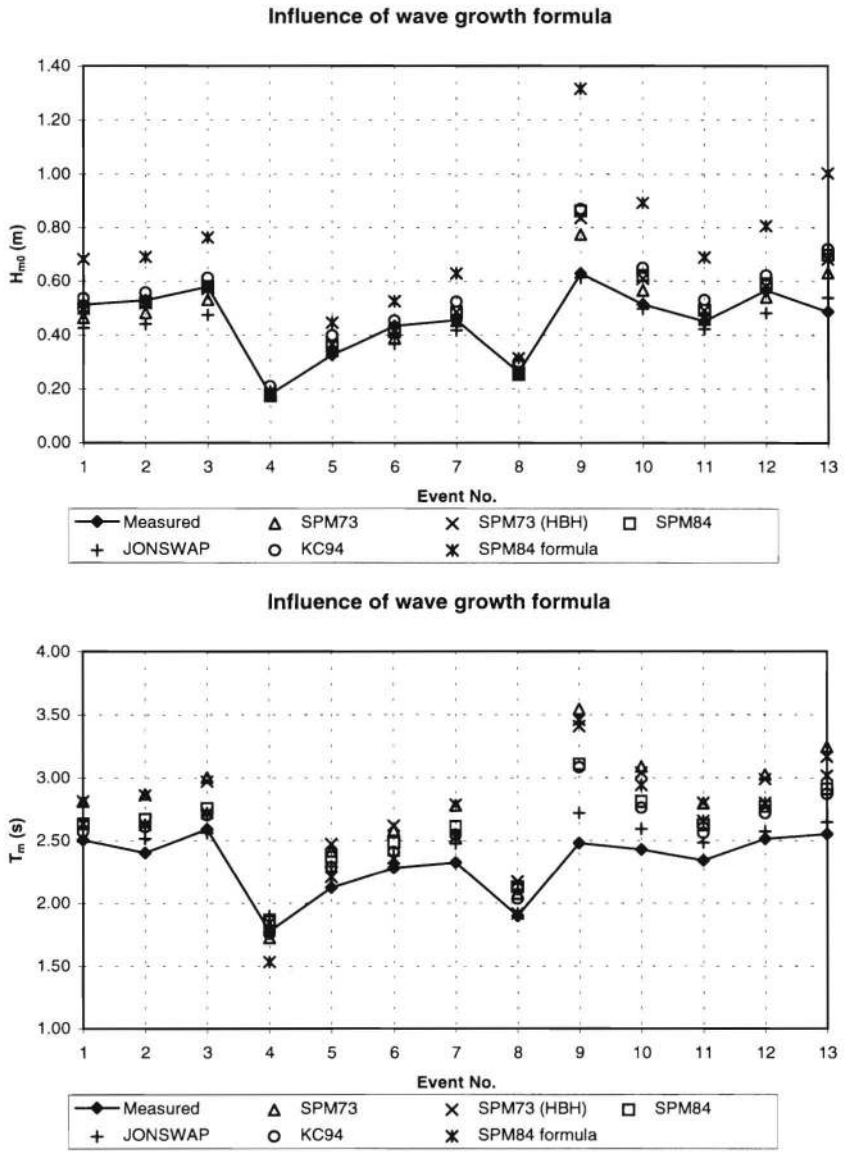

Figure 9. Comparison of measured significant wave heights (a) and mean periods (b) for different wind-wave growth source functions corresponding to different wave growth formulas.

can be obtained using the empirical information about the energy and peak frequency at full development from SPM84. Thus, $\tilde{E}_{fd} = 0.0037$ and $\tilde{\omega}_{p,fd} = 0.7725$. Using Eqs. 8–9 and 17a–17d, the coefficients a, b, c, d, $\tilde{t}_{mE}$ and $\tilde{t}_{m\Omega}$ are obtained for various deep water wave growth formulas and summarized in Table 1 for the mean JONSWAP spectrum ($\beta = 1.2$).

The use of empirical growth curves implies that the model implicitly include dissipation due to whitecapping (steepness related wave breaking in deep water). Hence, for deep water simulations, it should not be necessary to include additional wave dissipation in the model unless the implicitly included whitecapping dissipation for the wave growth curve used in formulating the source function is insufficient. In this case, additional steepness related wave breaking can be used as a means of calibrating the model by limiting the maximum steepness (calculated using the energy averaged mean frequency in Eq. 7) in deep water. Figure 1 shows typical results using coefficients corresponding to the KAHMA and CALKOEN (1994) growth formula for the ideal case of fetch limited wave growth in deep water. The wind speed, U_{10} is 10m/s and the mean wind direction is perpendicular to the coastline. The Kahma and Calkoen formula is plotted as full lines, while the model calculations is plotted as crosses. It can be seen that the model reasonably reproduce the underlying wind-wave growth formula as would be expected.

In shallow water, the input source function is calculated in the same way as for deep water, however, the shallow water dissipation terms (such as bottom friction and depth induced

Table 2. *Measured data and calculations using different wind-wave growth source functions corresponding to different wave growth formula. Values in the last two columns are obtained from direct calculation with SPM84 shallow water prediction formula. Bottom friction (k_N = 2 mm), depth induced breaking with γ_2 = 0.8.*

	Measured Data		SPM73		SPM73 (HBH coeff.)		SPM84		JONSWAP		KC94		SPM84-direct formula	
Event	H_{m0} Meter	T_m Secs	H_{m0} Meter	T_m Secs	H_{m0} Meter	T_m Secs	H_{m0} Meter	T_m Secs	H_{m0} Meter	T_m Secs	H_{m0} Meter	T_m Secs	H_{m0} Meter	T_m Secs
1	0.51	2.50	0.46	2.81	0.50	2.81	0.50	2.63	0.43	2.49	0.54	2.57	0.68	2.63
2	0.53	2.40	0.48	2.87	0.52	2.86	0.52	2.67	0.44	2.51	0.56	2.61	0.69	2.62
3	0.58	2.59	0.53	3.00	0.57	2.97	0.58	2.75	0.47	2.56	0.61	2.70	0.76	2.72
4	0.18	1.78	0.17	1.73	0.19	1.84	0.17	1.87	0.18	1.90	0.21	1.76	0.19	1.53
5	0.33	2.12	0.34	2.41	0.37	2.47	0.36	2.37	0.33	2.29	0.40	2.29	0.45	2.21
6	0.43	2.28	0.39	2.58	0.42	2.62	0.41	2.48	0.37	2.38	0.45	2.41	0.52	2.36
7	0.46	2.32	0.45	2.78	0.48	2.78	0.49	2.61	0.42	2.47	0.52	2.55	0.63	2.53
8	0.26	1.90	0.25	2.08	0.27	2.17	0.26	2.13	0.25	2.11	0.30	2.03	0.31	1.92
9	0.63	2.48	0.77	3.54	0.83	3.41	0.86	3.11	0.61	2.72	0.87	3.08	1.31	3.46
10	0.51	2.43	0.57	3.09	0.61	3.04	0.62	2.81	0.50	2.59	0.65	2.76	0.89	2.94
11	0.45	2.34	0.46	2.80	0.49	2.80	0.49	2.62	0.42	2.48	0.53	2.56	0.69	2.65
12	0.57	2.51	0.54	3.02	0.58	2.99	0.59	2.77	0.48	2.57	0.62	2.72	0.81	2.80
13	0.49	2.55	0.63	3.24	0.68	3.17	0.70	2.91	0.54	2.64	0.72	2.87	1.00	3.02
Root Mean Square Error =			0.06	0.51	0.08	0.48	0.09	0.30	0.06	0.14	0.11	0.25	0.30	0.37
Mean Error =			0.01	0.44	0.05	0.44	0.05	0.27	−0.04	0.12	0.08	0.21	0.23	0.24
Maximum Error =			0.15	1.07	0.21	0.93	0.23	0.63	0.10	0.24	0.24	0.60	0.69	0.98

wave breaking) may now be important. Furthermore, the propagation speeds c_{gx}, c_{gy} and c_θ are different in shallow water. Thus, wave growth in shallow water is governed by the balance between the input source function and the dissipation terms, and the changes in propagation speeds. For the ideal case of fetch limited wave growth in shallow water (depth = 5m), Figure 2 shows typical results using coefficients corresponding to the KAHMA and CALKOEN (1994) growth formula (indicated in the figure as KC94) compared to calculations using SPM84 shallow water wave growth formula. The wind speed, U_{10} is 10m/s and the mean wind direction is perpendicular to the coastline. In the numerical model, the geometric bed roughness is taken as 2mm (typical value), while the shallow water wave breaking parameter γ_2 is taken as 0.8 (typical value). For the SPM84 formula calculations, the wind speed is coverted to the wind stress factor, U_a which is used in the formula. However, results using the SPM84 shallow water wave growth formula is made dimensionless using the 10m wind speed, U_{10} (to be consistent with the numerical model results) and plotted as full lines in Figure 2. Although there is no reason to expect that the model calculations should agree with SPM84 shallow water formula, it is quite interesting that this is the case. This shows that this method recovers the results for the commonly used SPM84 shallow water equations under ideal conditions.

MEASURED DATA

Extensive wind and wave data were measured during 1994 at the Vindeby wind farm. The Vindeby wind farm is located between Langeland and Lolland, Denmark, with water depths varying from 2.1 m to 5.1 m, between the longitudes 11.09 to 11.16°E, and latitudes 54.96 to 54.98°N (BARTHELMIE *et al.*, 1994). Figures 3 and 4 (from BARTHELMIE *et al.* 1994) show the location of the wind farm. The measurements were collected and prepared by the department of meteorology and wind energy of Risø national laboratory, and made available for this study. Details about the instrumentation during the measurements can be found in BARTHELMIE *et al.* 1994.

The wind and wave data measured during April–May 1994 and Sep–Nov 1994 included the wind speed measured at 7 m above the mean sea level, U_7, the wind direction measured 20 m above the mean sea level, Dir20, the significant wave height derived from the wave spectrum, H_{m0}, and the energy-based mean wave period, T_m. The wind measurements were made from mast SMW (see Figure 4) located at 54.97°E, 11.13°N, while the wave measurements were sampled with an acoustic wave recorder about 20m from SMW.

The measured data were further analyzed to identify events that are suitable for modelling with MIKE 21 NSW, the results from which can then be compared with measured data. Since this model is a stationary model including wind-wave growth for fetch limited situations, the criteria used in identifying suitable events are:

(1) The waves must be generated by the local wind, *i.e.* negligible wave energy contribution from areas outside the study area. This is defined as a situation where the waves and the wind have a strong correlation with each other. The wave spectra is inspected to ensure that it is a single-peaked spectrum.
(2) Winds must be stationary. This is defined as a situation in which the wind speed and direction are relatively constant (within 10%) over a period of 3–4 hours. This period was chosen since preliminary computations using the *Shore Protection Manual* (1984) indicate that for winds of 5–10 m/s blowing from the west, for example, it takes about 3–4 hours for the wave climate to be fetch limited. It takes a shorter time for higher wind speeds.

The wind and wave data during the September/November campaign were divided into eight classes based on the wind direction. These are: 0 ± 22.5°, 45 ± 22.5°, etc. A plot of the significant wave height, H_{m0} versus the wind speed, U_7,

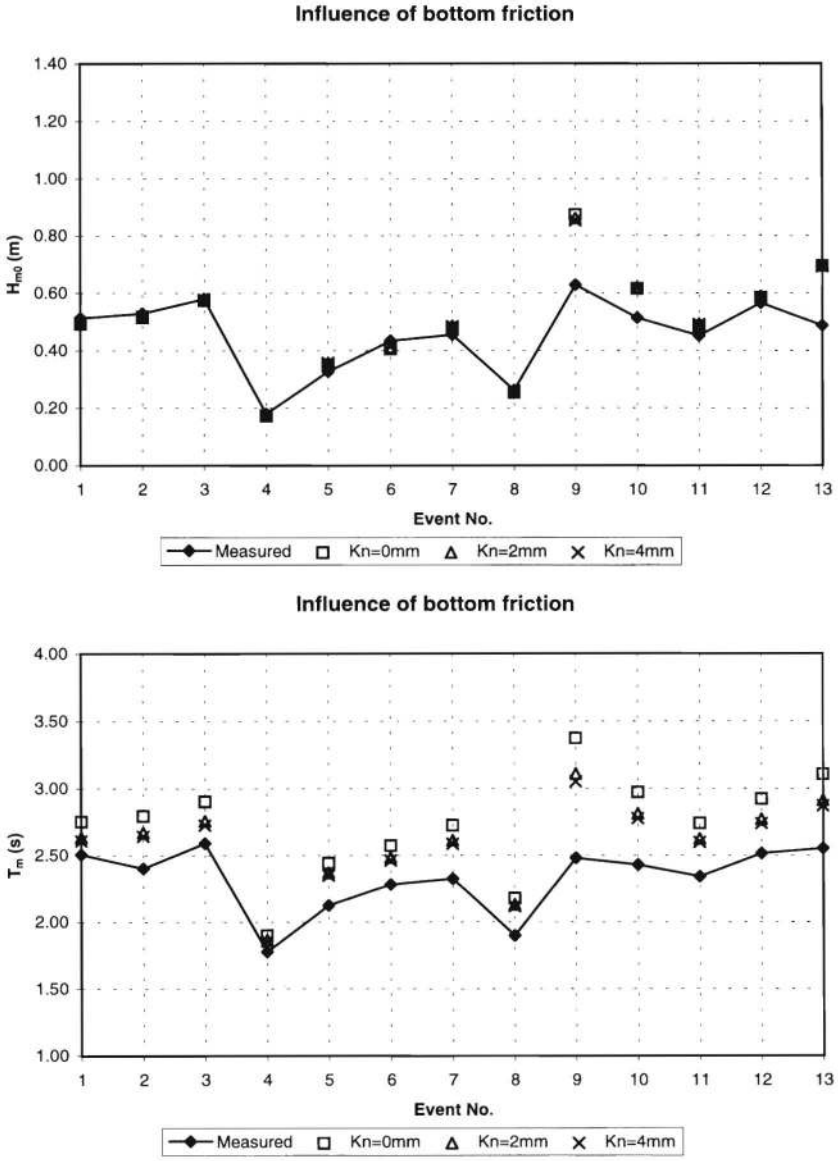

Figure 10. Influence of bottom friction on calculated wave climate. (a) Influence on significant wave heights (b) Influence on mean wave periods.

showed a strong correlation for each class, see for example Figure 5. This result indicates that the waves at the site are locally generated by the wind, *ie.* negligible influence of swell waves. Because of the difference in fetch lengths, the slope of the best fit line is different for each class. It is observed that for the longer fetches, the waves are higher for a given wind speed. For the purpose of these computations, we restrict ourselves to westerly winds (270°N ± 22.5°).

Using the second criterion, thirteen events were extracted from the data for westerly winds. For each event, the average measurement (arithmetic average of the measurements during the period) for the selected event was taken as representative of the measurement for that event. Figures 6a&b respectively show a plot of the wind speed and direction for all thirteen events. The central value for each event correspond to the mean value during the event, while the lower and upper values correspond to a spread of one standard deviation from the mean. Similar plots are shown in Figures 7a&b for the measured significant wave height and mean wave period. These plots indicate that the wind and wave conditions were reasonably constant for the selected events, with the possible exception of event No. 12. Thus, the data set is quite suitable for simulating with MIKE 21 NSW.

MODEL CALCULATIONS

A MIKE 21 NSW model of the study area was set up to do the wave growth calculations. The bathymetry of the study

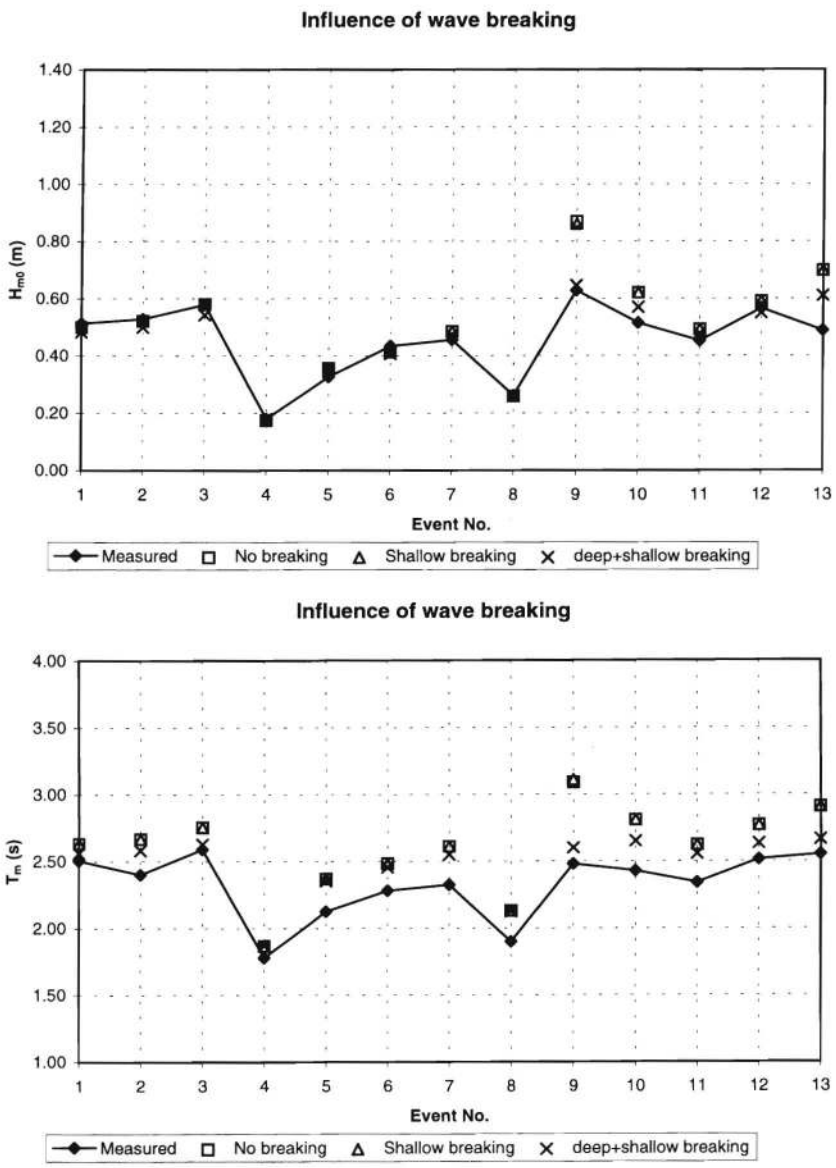

Figure 11. Influence of wave breaking on calculated wave climate. (top) Influence on significant wave heights (bottom) Influence on mean wave periods.

area is digitized from the Admiralty Chart No. 2597 (1991 edition). The digitized bathymetry is shown in Figure 8. The grid spacings are: $\Delta x = 50$ m, $\Delta y = 200$ m, with the x-direction corresponding to the main wave propagation direction. The directional distribution of the wave energy within $\pm 60°$ of the x-direction was resolved with 13 discrete directions, using a grid spacing $\Delta\theta = 10°$.

For these simulations, the wind speed at 10m elevation, U_{10} is calculated using the 1/7 power law suggested in SPM84 for correcting wind speeds at elevations less than 20 m. The wind direction at 20 m is assumed to be valid at 10m. Furthermore, atmospheric stability correction was not applied for these simulations, since all the events were in the near-neutral atmospheric stability range.

First, we investigate the effect of land-water roughness change on the wind speeds, since it can be argued that one should use the 'average' wind speed over the fetch, rather than wind speed measured at one location. For this purpose, we use the method of TAYLOR and LEE (1984) (cited by VERHAGEN and YOUNG, 1994). Consider a change of surface roughness from land to water. According to Taylor and Lee, this change creates an internal boundary layer. The thickness of this internal boundary layer varies with fetch and is given by:

$$\delta_i = 0.75 z_o \left(\frac{x}{z_o}\right)^{0.8} \tag{18}$$

where z_0 is the aerodynamic roughness of the water surface and x is the distance from the land boundary (fetch). Outside the

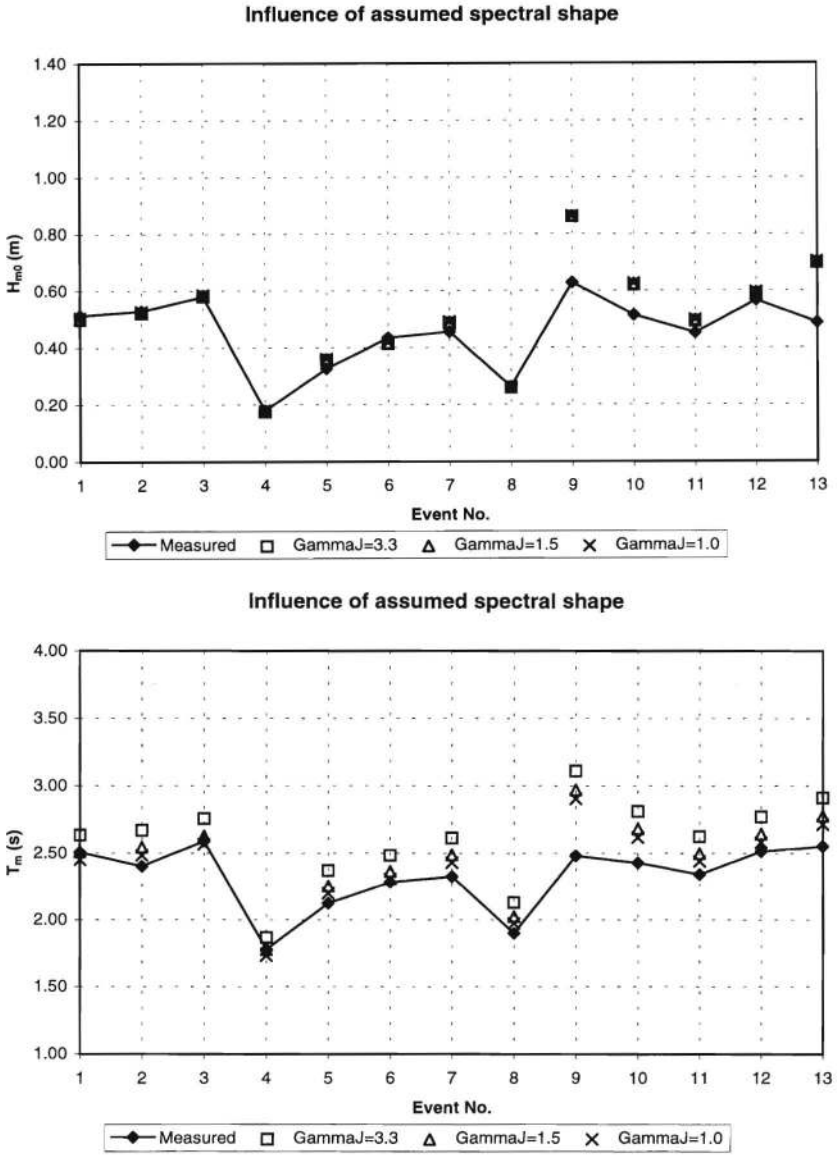

Figure 12. Influence of JONSWAP peakedness parameter (assumed spectral shape) on calculated wave climate. (a) Influence on significant wave heights (b) Influence on mean wave periods.

internal boundary layer, the overwater wind speed is given by the usual logarithmic profile, while a modified expression is used inside the boundary layer. The expressions are given below:

$$U_{water}(z) = \frac{u_*}{\kappa}\ln\left(\frac{z}{z_o}\right) \qquad z \geq \delta_i \tag{19}$$

$$U_{water}(z) = \frac{\ln\left(\frac{z}{z_o}\right)\ln\left(\frac{\delta_i}{z_{land}}\right)}{\ln\left(\frac{\delta_i}{z_o}\right)\ln\left(\frac{z}{z_{land}}\right)}U_{land}(z) \qquad z < \delta_i \tag{20}$$

where u_* is the wind friction speed, κ is the von Karman constant taken as 0.4, z is the elevation from sea level, z_o is the sea roughness and z_{land}, U_{land} are respectively the aerodynamic roughness and wind speed over land. In the application of Eqs. 18 and 20, z_o and z_{land} were assumed to be 0.00035 m and 0.15 m respectively. Note that z_{land} = 0.15 m is a typical value for the aerodynamic roughness over land areas (LARSEN, S.E., 1993), z_o is commonly calculated using the Charnock relationship, viz: $z_o = \alpha u_*^2/g$ where α is typically 0.0185 and u_* is the wind friction velocity which is dependent on the wind speed. For a mean wind speed of 10 m/s, and using $u_* \approx U_{10}/30$, z_o is estimated as 0.35mm.

Using Eqs. 18 and 20, we calculated the ratio $R = U_{water}/$

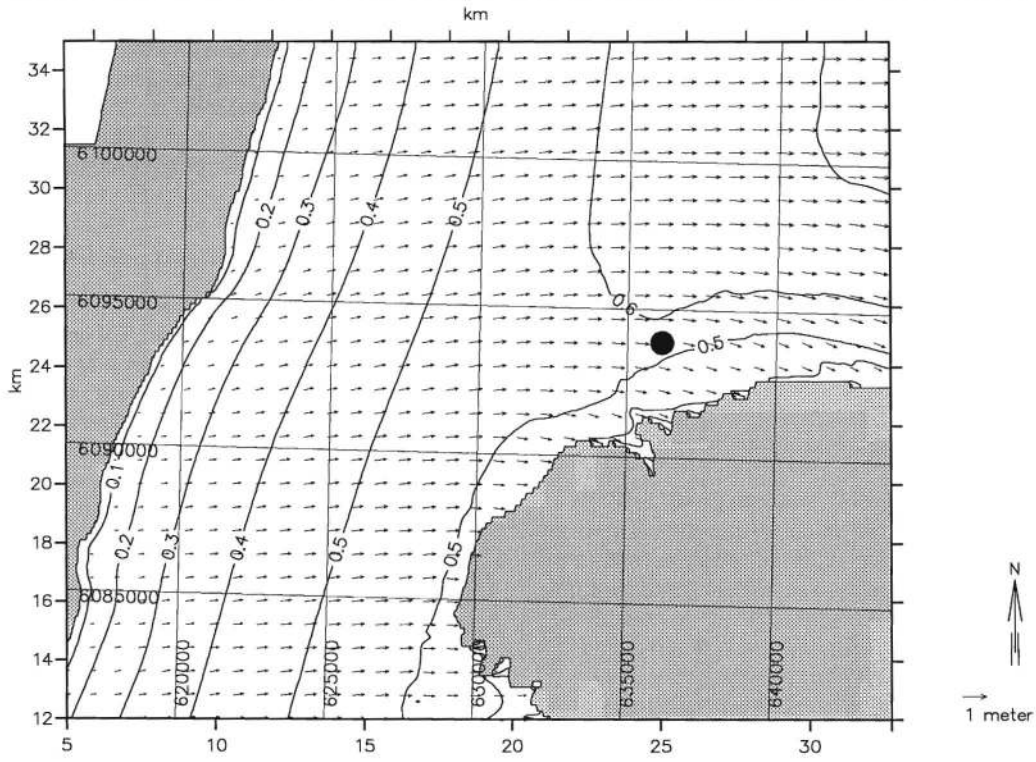

Figure 13. Illustration of typical 2D variation of significant wave heights and direction calculated with the model using KAHMA and CALKOEN (1994) coefficients for Event 1. Heavy black dot indicates wave measurement location.

U_{land} at 1 km increments up to 25 km. The values of R are now averaged and compared with the value at 20 km fetch (approximate fetch for the westerly winds) to obtain a correction factor for the wind speed to be used in the model. The correction factor was found to be about 0.97, which is very close to 1.0. Thus, the measured wind speed (measured at approximately 20km fetch) was taken to be an adequate representation of the "average" wind speed over the fetch.

Several simulations were carried out in order to investigate the following: a) Influence of deepwater wave growth curve, b) Influence of wave breaking, c) Influence of bottom friction d) Influence of assumed spectral shape.

Influence of Wave Growth Formula Used in Source Function

In order to assess the influence of different deep water wave growth formulas used in the source function for wind-wave growth, we simulated the thirteen events using coefficients corresponding to different formulas summarized in Table 1. In addition, we also use the coefficients given by HBH which is tuned to the SPM73 growth formula. In all, we investigated the use of the following formulas: 1) SPM73 (Table 1); 2) SPM73 (coefficients fitted by HBH); 3) SPM84; 4) JONSWAP (same coefficients as SPM84); 5) KAHMA and CALKOEN (1994). The wind speed at 10m elevation U_{10}, is used in all the above cases, except in the case of SPM84 coefficients where the wind stress factor is used. For these simulations, the influence of bottom friction was included with a typical geometric bed roughness, k_N of 2mm. The influence of bottom friction on wave period was also included. In addition, the influence of depth induced wave breaking on wave energy was included with γ_2 set to 0.8.

For comparison with numerical model results, calculations using the SPM84 shallow water wave prediction formula is also used. In applying this formula, the wind speed for each event is converted to the wind stress factor U_a used in the formula. Furthermore, the upwind fetch corresponding to the wind direction and the average water depth along the fetch are used.

The results are shown in Figure 9a (significant wave heights, H_{m0}) and Figure 9b (energy averaged mean wave period, T_m) and in Table 2. Calculations using the SPM84 shallow water formula directly consistently overpredict the wave heights. This is probably due to the following factors: (a) the formula is unable to account for the variability in the water depths. This variability in water depths leads to wave refraction, which refracts some wave energy away from the measurement site. (b) the formula is unable to take into consideration the directional spreading in the wind and the consequent changes in fetch along different discrete directions.

With the numerical model, the JONSWAP coefficients gives the best result in terms of low root mean square errors, however, it has the undesirable tendency to underpredict the

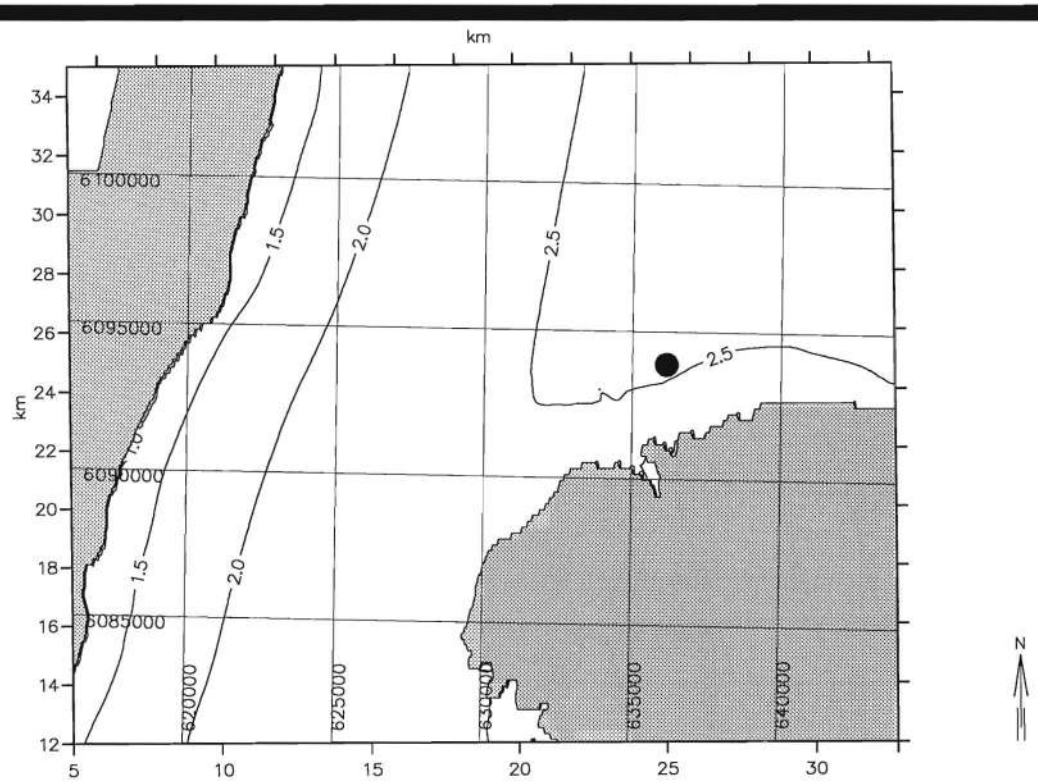

Figure 14. Illustration of typical 2D variation of mean wave period, T_m calculated with the model using KAHMA and CALKOEN (1994) coefficients for Event 1. Heavy black dot indicates wave measurement location.

wave heights. The SPM73 coefficients also give a good prediction for the wave height, but it gives poor results (compared to the others) for wave period. The SPM84 and KAHMA and CALKOEN (1994) coefficients gives generally good results for wave heights and periods. It is difficult to choose between the two, SPM84 gives slightly better results for wave heights, while Kahma and Calkoen is slightly better for the wave periods. Thus, the overall best results for H_{m0} and T_m were obtained using the SPM(1984) or the KAHMA and CALKOEN (1994) coefficients in the source function.

Influence of Bottom Friction

In order to assess the influence of bottom friction on the wave field, the model setup was used with the SPM84 coefficients. Three different values of geometric bed roughness viz: k_N = 0 mm, 2 mm and 4 mm were investigated. The results of these simulations are shown in Figure 10. Figure 10 shows that the calculated wave heights are not significantly sensitive to bottom friction. At first glance, this may look surprising, since the measurement site is relatively shallow (depths about 3 to 4 m). However, when one considers that waves at the site are fetch-limited, (fetch for westerly winds ~ 20 km), hence for the typical wind speeds encountered during the field campaign (U_{10} ~ 10 m/s), the waves are actually closer to deep water waves than to shallow water waves ($k_p d \sim 2.5$). Thus, the waves don't quite feel the bottom as for shallow water waves. Furthermore, the depth along the fetch is relatively deeper, about 12 m on average. Since bottom friction is usually important only after wave propagation over a large distance where the waves feel the bottom, it is not surprising that this effect is unimportant in this case. This explains the relative insensitivity of the predicted wave heights to bottom friction. However, there is a small influence on the energy averaged mean wave period up to k_N of 2 mm, above which the influence is no longer noticeable.

Influence of Wave Breaking

To assess the influence of wave breaking, three sets of simulations were carried out. This correspond to the situation with no wave breaking, with only shallow water wave breaking and with combined shallow and deep water wave breaking. In all the simulations, the SPM84 coefficients were used. The parameters governing wave breaking were set as: γ_1=1.0 (maximum steepness parameter) and γ_2=0.8 (maximum H/d parameter; H is wave height and d is water depth). This corresponds to the values suggested in HBH.

The results are shown in Figures 11a and 11b. It is seen from Figure 11 that the wave height and period is not affected by shallow water breaking. In fact, apart from events 9 and 13 with relatively high wind speeds (U_{10} > 12m/s), the results are already very good without the inclusion of wave breaking. This is not quite as surprising as it would look at first glance, if one recognises that the ratio of the significant wave height to water depth (H_{m0}/d) at the site is less than

0.2. For events 9 and 13, additional deep water breaking (additional to what is implicitly included in the SPM84 wave growth formula) is required to bring the wave height and period closer to the measurement. The root mean square error (RMSE)[2] for H_{m0} and T_m is calculated as (10 cm, 0.30 s), (9 cm, 0.30s) and (4 cm, 0.17s) for the cases with no breaking, depth induced breaking and combined shallow & deep water breaking respectively.

Influence of Assumed Spectral Shape

Recall that in Eqs 17a–d, we need to specify the ratio (β) between the peak period, T_p and the energy averaged mean period, T_m. This ratio is a function of the assumed shape of the wave spectrum. For the purpose of this study, we assume a generic JONSWAP shape with standard coefficients, except for the peakedness parameter (γ_J) which is allowed to vary. Thus, for the same energy and peak period, the broadness or peakedness of the spectrum will be governed by γ_J. Thus, β is also governed by γ_J.

From the results presented in Figures 9–11, the mean wave period is generally over-predicted. This is probably related to the use of $\beta = 1.2$ corresponding to mean JONSWAP ($\gamma_J = 3.3$) in the model. Analysis of the measured spectra for the thirteen events indicated a peakedness parameter lower than 3.3, varying between 0.5 and 2.5, with a mean γ_J of about 1.5. Intuitively, this implies that the mean frequency will be higher for this less peaked spectrum than for a mean JONSWAP. Thus, the mean period will be lower than for a mean JONSWAP, which seems to explain the over-prediction of the wave period in the model. To test this reasoning, simulations were carried out using $\gamma_J = 3.3$, 1.5 and 1.0, corresponding to $\beta = 1.20$, 1.26 and 1.28 respectively). For these simulations, the same model setup as in section 4.1 was used, with the SPM84 coefficients. The results are shown in Fig. 12. As expected, the energy averaged mean wave period was reduced closer to the measured values with reducing γ_J, while the calculated significant wave heights are not sensitive to the value of γ_J.

It is noted that if deep water wave breaking is included in the simulation, there will be a general reduction in the wave heights. This is due to the increased importance of the steepness breaking criterion when the energy averaged mean period reduces, which leads to a reduction of the maximum wave height H_m. This is not the case here, because the simulations were carried out including only depth-induced breaking (shallow water breaking).

A typical illustration of the spatial variation in the significant wave height and energy averaged mean period is shown in Figures 13 and 14 respectively for Event 1 ($U_{10} = 9.1$ m/s, Direction = 271°N). In these plots, the growth of the waves with increasing fetch can be observed. It is also observed that the mean wave direction in the central part of the model is slightly turned with respect to the wind direction, and tends towards the direction of maximum fetch. This tendency for waves in restricted fetches to tend towards the direction of maximum fetch has been observed in nature, see for example DONELAN (1980).

Closer to the shoreline of Lolland (the eastern land mass in the model), the waves turn towards the shoreline. This phenomenon is partly caused by refraction, but more importantly (for this case with relatively short waves), the turning is caused by the sheltering effect of Lolland. This sheltering leads to a reduction in the contribution to total wave energy for some discrete directions (directions $\leq$ 270°N) in the $\cos^2$ directional spreading function used for the wind-generated waves. Thus, the mean wind direction shifts towards higher directions. This phenomenon is different from refraction, which is caused by changes in the propagation speeds.

CONCLUSIONS

(1) The simulations of Vindeby data show that the approach introduced by HBH for computing locally generated wind waves performs quite well for this shallow and fetch limited situation. The model gave better results than a direct application of the SPM84 shallow water prediction formula.

(2) Of the 5 wave growth formulas investigated for the source function, the overall best results for H_{m0} and T_m were obtained using the SPM (1984) or the KAHMA and CALKOEN (1994) coefficients. The JONSWAP coefficients gives a better root mean square error than SPM (1984) or KAHMA and CALKOEN (1994), however, it has the undesirable tendency to under-predict the wave heights at this site. The SPM (1973) coefficients also give a reasonable prediction for the wave height, but results for wave period is not as good (compared to the other formulas).

(3) The Vindeby simulations show that in areas with relatively short fetches (Fetch of about 20 km) and apparently shallow water, (depths of about 3 to 4 m at the measurement site), the waves generated by the local wind behave essentially like deep water waves, since they are relatively short period waves which do not feel the bottom. The influence of shallow water wave breaking and bottom friction was found to be insensitive to the calculated significant wave heights. For the simulations with strong winds, additional deep water wave breaking is required in order to bring the calculations closer to measured data.

(4) Furthermore, the accuracy of the predicted mean wave period was found to depend on the assumed spectral shape in the model formulation. Using a JONSWAP spectrum with a peakedness parameter of 1–1.5 (comparable to the peakedness parameter obtained from the measurements) gave slightly better results than using the mean JONSWAP value of 3.3. However, this requires that steepness related breaking should not be included in the analysis.

ACKNOWLEDGEMENTS

This work was funded by the Danish Technical Research Council (STVF) as part of the project "Wind-Wave Interaction in Coastal and Shallow Areas" carried out in collaboration with the Department of meteorology and wind energy of Risø National Laboratory. The measured data used here was col-

[2] The root mean square error (RMSE) is calculated thus:

$$\mathrm{RMSE} = \frac{1}{13}\sum_{i=1}^{13}(H_{m0,i} - H_{m0,\mathrm{observed}})^2$$

lected by Risø National Laboratory as part of the RASEX experiment and made available for this study by Messrs J. Højstrup and S. Larsen. This is gratefully acknowledged. Stimulating discussions with Messrs Ole R. Sørensen, Hans Jacob Vested and Henrik Kofoed-Hansen on this paper are acknowledged. The useful comments by the reviewers are also gratefully acknowledged.

LITERATURE CITED

BARTHELMIE, R.J.; COURTNEY, M.S.; HØJSTRUP, J., and SANDERHOFF, P., 1994. The Vindeby Project: A Description, *Report Risø-R-741 (EN)*. Risø National Laboratory, Roskilde, Denmark.

BATTJES, J.A. and JANSSEN, J.P.F.M., 1978. Energy loss and set-up due to breaking in random waves, *Proceedings of the 16th International Conference on Coastal Engineering* (ASCE), pp. 569–587.

BISHOP, C.T.; DONELAN, M.A., and KAHMA, K.K., 1992. Shore protection manual's wave prediction reviewed. *Coastal Engineering*, 17, 25–48.

DONELAN, M.A., 1980. Similarity theory, applied to the forecasting of wave heights, periods and directions, *Proceedings Canadian Coastal Conference*, 1980, National Research Council Canada, pp. 47–61.

DINGEMANS, M.W., 1983. Verification of numerical wave equation models with field measurements, CREDIZ verification Haringvliet. *Delft Hydraulics Lab., Rep.No. W488*, Delft, 137p.

GODA, Y., 1974. Estimation of wave statistics from special information. *In: Proceedings International Symposium Ocean Wave Measurement and Analysis (WAVES '74)*. ASCE. pp. 320–337.

HASSELMANN, K.; BARNETT, T.P.; BOUWS, E.; CARLSON, H.; CARTWRIGHT, D.E.; ENKE, K.; EWING, J.A.; GIENAPP, H.; HASSELMANN, D.E.; KRUSEMAN, P.; MEERBURG, A.; MUELLER, P.; OLBERS, D.J.; RICHTER, K.; SELL, W., and WALDEN, H., 1973. Measurements of wind-wave growth and swell decay during the Joint North Sea Wave Project (Jonswap). *Dtsch. Hydrogr. Z.*, 121–195.

HOLTHUIJSEN, L.H.; BOOIJ, N., and HERBERS, T.H.C., 1989. A prediction model for stationary, short-crested waves in shallow water with ambient current. *Coastal Engrg.*, 13, 23–54.

JONSSON, I.G., 1966. Wave boundary layers and friction factors. *Proceedings 10th Conference on Coastal Engineering* (ASCE), 1967, 1, 127–148.

KAHMA, K.K., and CALKOEN, C.J., 1994. Growth curve observations. *In:* KOMEN *et al., Dynamics and Modelling of Ocean Waves*. Cambridge University Press. pp. 174–182.

KOMEN, G.J., CAVALERI, L., DONELAN, M., HASSELMANN, K., HASSELMAN, S., and JANSSEN, P.A.E.M. 1994. *Dynamics and Modelling of Ocean Waves. Cambridge University Press*, 532p.

LARSEN, S.E., 1993. Observing and modelling the planetary boundary layer. *In:* E. RASCHKE and D. JACOB. (eds.) *NATO ASI Series, Vol. I 5, Energy and Water Cycles in the Climate System*. Berlin: Springer-Verlag.

MICHE, R., 1944. Mouvements ondulatoires de la mer en profondeur constante ou décroissante *Ann. Ponts Chausees*, 114, 369–406 (cited by Holthuijsen *et al.*, 1989).

Shore Protection Manual, 1973. 3 Vols. US Army Engineer Waterways Experiment Station, Coastal Engineering Research Center, Vicksburg, Massachussetts.

Shore Protection Manual, 1984, 2 Vols., 4th edition, US Army Engineer Waterways Experiment Station, Coastal Engineering Research Center, Vicksburg, Massachussetts.

TAYLOR, P.A. and LEE, R.J., 1984. Simple guidelines for estimating wind speed variations due to small scale topographic features. *Climatological Bulletin*, 18(2), 3–32 (cited by Verhagen and Young, 1994).

VERHAGEN, L.A. and YOUNG, I.R., 1994. The growth of wind waves in shallow water, *24th International Conference on Coastal Engineering* (Kobe, Japan), pp.665–673.